Influence of silica nanoparticles on corrosion resistance of sol-gel based coatings on mild steel

Laura VIVAR MORA[1, 4], Sanjeev NAIK[2], Shiladitya PAUL[2], Richard DAWSON[3], Anne NEVILLE[4], Richard BARKER[4]

[1]National Structural Integrity Research Centre (NSIRC), United Kingdom
mnlvm@leeds.ac.uk
[2]TWI Ltd., United Kingdom
[3] *Lloyd's Register EMEA,* Southampton Technical Support Office, Marine & Offshore, United Kingdom
[4] Institute of Functional Surfaces, School of Mechanical Engineering, University of Leeds, United Kingdom

Abstract:

For this study, unfunctionalised and functionalised nanoparticles of silica (SiO_2) were incorporated into a sol-gel based matrix in an effort to provide more effective corrosion protection on a mild steel substrate. Tests such as atomic force microscopy (AFM) and white light interferometry (WLI) were carried out to characterise coating microstructure and properties. Corrosion protection and coating durability was investigated using different methods which included electrochemical impedance spectroscopy (EIS) and accelerated salt spray testing to simulate a marine environment. Electrochemical test results as well as results after exposure in the neutral salt spray test indicated that the addition of silica nanoparticles led to an improvement in corrosion resistance of the coating matrix. The most effective performance was observed when the nanoparticles were functionalised. Nanoparticle functionalisation helped to avoid agglomeration during incorporation leading to a more uniform nanoparticle distribution within the coating formulation and an improvement of the coating's ability to protect against corrosion.

Highlights:

- The influence of silica (SiO_2) nanoparticle incorporation in a sol-gel based coating was studied
- SiO_2 particle surface treatment improved coating homogeneity and prevented cracking propagation
- Corrosion resistance improved with functionalised SiO_2 nanoparticles

Keywords:

polysiloxane coatings, sol-gel, silica nanoparticles, nanoparticle surface treatment, corrosion protection

1. Introduction

Corrosion has a significant economic as well as environmental impact on almost all the world's infrastructure. One of the most widely used materials in infrastructure is carbon steel, mainly because of its versatility, durability and affordability. The corrosion of carbon steel as a result of electrochemical reactions in its service environment is a spontaneous process which can, if no measures are taken to prevent or control it, compromise material integrity and impact not only the asset but also the environment and people.

The most common method of mitigating corrosion of carbon steel is the use of specialised coatings, mainly organic coatings (such as epoxies, polyurethanes, acrylics) and inorganic coatings (such as polysiloxanes). Combining the benefits of organic and inorganic compounds to design hybrid protective coatings is still a challenge for industrial application. Inorganic coatings have advantages, but purely inorganic siloxane based coatings are tough to use for industrial applications unless used at very low thicknesses (<1-2 microns). Hence, most industrial applications try to combine polysiloxanes with epoxies or acrylics to give hybrid resins like epoxy-siloxane hybrids or acrylic-siloxane hybrids. One route to create these types of coatings is the sol-gel process, which involves hydrolysis and condensation of metal alkoxides (precursors) in the presence of acid or base as a catalyst [1-3]. The resulting oxide materials present structures vary in range from nanoparticulate sols to continuous polymer gels, depending on the rate of each of these reactions and subsequent drying and processing steps. A hybrid coating possesses an organic part, which imparts flexibility and impact resistance, and an inorganic part, which usually helps to decrease porosity and increase homogeneity and thickness [4, 5].

Coatings based on tetraethylorthosilicate (TEOS) and a second silane have been used to protect many different substrates such as aluminium/aluminium alloys [6-9], magnesium alloys [10], and steel [11, 12]. In all the studies, improvement of the corrosion resistance of the

coatings was reported with the second silane. Different parameters affect the final performance of these sol-gel based coatings, such as amount of water, type and amount of catalyst, temperature, and the protocols followed to achieve a proper balance of hydrolysis and condensation reactions. Thus, careful choice of reaction and processing parameters is important to obtain protective hybrid coatings by the sol-gel route. Porosity and tendency to crack due to the high stress in a cured sol-gel coating can contribute to lowered performances when it comes to resistance against corrosion.

One of the promising routes to develop high performance corrosion resistant systems is through the use of nanotechnology. Nano-additives can be used in many different ways; as layered nanomaterials (graphene, clays or layered hydroxides), metal oxides (silica, ceria or titania), or as nanocontainers containing active corrosion inhibitors which are released in response to a stimuli. Previous work has shown that the use of nano-additives can aid corrosion protection as well as lead to more durable coatings [13, 14], with improved mechanical and barrier properties [15-24], scratch resistance and a lower tendency for blistering and delamination [20, 25, 26].

Research has reported that the addition of nanoparticles helps to increase thickness of the films [5, 9, 27], and improve mechanical and barrier properties leading to corrosion resistance [6, 7, 12, 28, 29]. However, in order to develop high performance coatings with nano-additives, it is important to incorporate an optimum loading level of nanoparticles with the appropriate surface chemistry to provide good compatibility and dispersion in the base coating matrix. Agglomeration of the nanoparticles in the coating matrix can not only prevent adequate corrosion protection, but can in some cases lead to an inferior performance even compared to the base matrix due to the introduction of defects.

The aim of the present work is to create a sol-gel based coating and modify it with silica nanoparticles to study their interaction with the coating matrix and the influence of these nanoparticles on the barrier properties of the coating.

The surface of a silica nanoparticle is highly hydroxylated with silanol groups. These groups have a significant impact on the surface charge of silica nanoparticles and agglomeration of the nanoparticles. In addition, they also provide an opportunity to functionalise the silica nanoparticles with various functional groups. It has been widely reported that surface treatment of silica nanoparticles can be tailored to enhance the affinity between organic and inorganic phases in a nanocomposite and improve the dispersion of nanoparticles within the resin matrix [18]. The ultimate objective of this study is to understand the impact of as-synthesised unfunctionalised as well as suitably functionalised silica nanoparticles on the corrosion protection of carbon steel using these coatings.

2. Experimental

2.1 Materials

Q-panels (Q-Lab Company, UK), grade S-46 (A1008 steel), ground on one side with dimensions of 0.8 x 102 x 152 mm were used as the substrate. TES40, an oligomeric form of TEOS, and 3-glycidoxypropyltrimethoxysilane (GPTMS) precursors were supplied by Silanes and Silicones Manufacturing, UK. The synthesis of silica nanoparticles was carried out at TWI Ltd., Cambridge, by a standard Stöber method [1].

2.2 Coating preparation

2.2.1 Sol-gel based coatings

This study started with TES40, which is the oligomeric form of TEOS. However, when used alone it was difficult to create a film-forming coating. Pure inorganic films with thickness higher than a few microns are usually not easily formed using sol-gel chemistry and are fragile and crack easily. Thus, a second silane, 3-GPTMS (3-glycidoxypropyltrimethoxysilane), was

added to the formulation to help with the formation of the matrix. This precursor has two components, one non-hydrolisable glycidyl ligand (organic) and three hydrolysable methoxy ligands, with all ligands being attached to a central silicon atom. The combination of these precursors, TES40 and GPTMS, was used to develop a coating matrix. Organic-inorganic coatings were prepared using TES40 and GPTMS as precursors in the presence of acidic catalyst of HCl with water and Industrial Methyl Spirit (IMS) as solvents.

Three different TES40/GPTMS molar ratios (1:0.6, 1:0.9 and 1:1.8) were tried in order to create a film-forming coating with a thickness greater than a few microns to which nanoparticles can then be added. Some of these combinations are detailed below in Table 1.

2.2.2 Silica nanoparticles: Preparation and incorporation in coating

Silica nanoparticles for this study were prepared by the Stöber process [1], which produces mono-modal spherical silica nanoparticles by an ammonia catalysed reaction of tetraethoxysilane (TEOS) in alcohols as solvent. The Stöber silica dispersion made at TWI is a 4.3 wt.% dispersion in IMS (Industrial Methylated Spirit), with the silica nanoparticles having a mono-modal distribution with a mean particle size (Z-average, as measured by dynamic light scattering, DLS, Malvern Zetasizer Nano ZEN1600) of 25 nm.

After synthesis of the silica nanoparticles, the ammonia was removed by evaporation in a rotovap. IMS was introduced to maintain a constant weight of 4.3 wt.% silica during the process. The final output was a suspension that was translucent (slightly blue haze) with a pH of ~8-8.5. This suspension was added to the TES40. The solvent was removed by using a rotovap until the solvent content was <10-15 wt.% and the SiO_2 (particle) content was 10wt.%. This mixture was used then as a component in the matrix formulation.

Silica nanoparticles were introduced into the optimised formulation with the TES40/GPTMS molar ratio of 1:1.8. It was expected that incorporation of these nanoparticles to an optimum

loading level would help to increase the thickness, improve mechanical properties and corrosion resistance of the coating. It can also have the opposite effect if overloaded [27].

2.2.3 Silica particles: Surface functionalisation

In a second variant, the silica nanoparticles were surface-treated with GPTMS to make them more compatible with the matrix and to prevent/reduce agglomeration of nanoparticles during incorporation into the coating formulation. Surface functionalisation of the synthesised silica nanoparticles with GPTMS was carried out by reacting 100 g of silica dispersion prepared by the Stöber method (as described in section 2.2.2) with 0.43 g of GPTMS, giving a mass ratio of 0.1 g GPTMS/g silica in the dispersion. This solution was stirred for a few minutes and then heated to 65°C for 18 h. No added water was used to promote functionalisation as it is anticipated alcohol liberating reaction between the GPTMS and the silanols on the silica particles surface would facilitate functionalisation.

The acidity (pH value) of the solution was adjusted with acetic acid to be between 3-5 to facilitate the hydrolysis and subsequent reaction of the GPTMS with the silanol groups. Maintaining acidic pH is important since previous researchers have demonstrated that alkaline conditions (pH 9.9) leads to the formation of aggregates after surface modification, while modified silica at pH 2.6 remains monodisperse with no large aggregation observed [30].

Following the same method as described earlier, the functionalised silica dispersion was added to the matrix formulation to a 10 wt.% loading level. Figure 1 shows the hydrolysis of GPTMS and the subsequent functionalisation of the silica surface.

2.3 Coating procedure

Prior to coating deposition, steel panels were cleaned with IMS to remove grease and/or contaminants. Coatings were applied manually using 50 µm wire wound bars on to the steel panels (Elcometer, Manchester, UK). The coated samples were then dried and cured at 90°C for 2 h in an oven.

2.4 Coating characterisation

The coating thickness was measured using an Elcometer 456 Eddy current coating thickness gauge (Elcometer, Manchester, UK). At least five measurements were made at five different locations on each sample. The average and standard deviation of the film thickness for each of the tested coatings were calculated to ensure consistency across the coated surface.

Adhesion of the coating to the substrate was measured by the cross-cut tape test method following ASTM D3359 - 09e2.

Atomic Force Microscope (AFM) images were obtained using a Dimension Icon (Bruker, Germany) operating in Peakforce Quantitative Nano-mechanical mapping mode using a silicon tip on a nitride cantilever probe (Bruker, nominal spring constant 0.4974 N/m, nominal resonance frequency of 70 kHz).

The Neutral Salt Spray Test (NSST) was used as a rapid screening test to evaluate the corrosion protection of the coatings. The test was run in a salt spray chamber (Ascott CC1000ip, Ascott, UK) following ASTM B117. Corrosion resistance of the coated samples was examined by exposing them to a salt fog atmosphere generated by spraying a 5 wt.% aqueous NaCl solution at 35±2 °C. Prior to exposure, the back and the edges of the samples were covered with lacquer. Specimens were inspected after 24 h, 48 h, and 72 h of exposure to assess performance.

A 3D White Light Interferometer (WLI, Bruker Contour GT-K 3D Optical Microscope) was used to record three-dimensional surface topographies of coatings while Differential Interference Contrast microscopy (DIC, Nikon Optiphot Microscope) was used to gather information about possible invisible features in the coatings.

The coatings were also evaluated by electrochemical measurements, which were performed using a conventional three-electrode cell with 3.5 wt.% NaCl electrolyte at ambient conditions. The working electrode was the coated sample (exposed area 15.2 cm^2), the reference electrode was Ag/AgCl (4M KCl) type and the counter electrode was a Pt/Ti wire. The corrosion

potential, electrochemical impedance spectroscopy (EIS) and Tafel polarisation characteristics were measured using an Ivium pocketSTAT (Ivium, Netherlands). The EIS measurements were performed at the OCP in the frequency range 10 kHz-0.005 Hz with perturbation amplitude of ±20 mV. The data was analysed using ZView software (Scribner, USA). Constant phase elements (Q) were used in all fittings instead of capacitances considering the non-ideal capacitance behaviour of the system. The impedance of Q is defined by the following equation [31]:

$$Z(j\omega) = (Y_0)^{-1}(j\omega)^{-n} \qquad (1)$$

where, ω is the angular frequency, Y_0 is the Q constant and n is a value which represents the deviation from purely capacitive behaviour ($0 \leq n \leq 1$). In the case of an ideal resistor or capacitor, n=0 or 1 respectively.

EIS measurements were carried out since they can provide insight of the physicochemical processes on the coated substrate during corrosion, which can help to explain the corrosion behaviour observed during salt spray testing.

3. Results and discussion

3.1 Coating microstructure

The measured thicknesses for the three different TES40/GPTMS molar ratios (1:0.6, 1:0.9 and1:1.8) were found to be around 10-12 µm for 1:0.6 and 1:0.9 molar ratios while the 1:1.8 increased to around 30-40 µm. It was found that increasing the organic content (via the glycidyl group of the GPTMS) in the sol-gel based matrix formulation helped to improve the adhesion of the coating to the substrate as well as provide more uniform and thicker coatings, which is in agreement with other studies [32, 33]. Thus, a TES40/GPTMS molar ratio of 1:1.8 was selected as the preferred matrix formulation due to its uniformity, its lower susceptibility to cracking and its enhanced thickness.

Coating thickness for the preferred matrix and the matrix with incorporated silica was measured to be 20-40 µm for various samples. Adhesion of the coating to the substrate measured by the cross-cut tape test method gave a 5B rating (rating adhesion with 0B to 5B scale) for all samples, meaning that all coating formulations were well adhered to the substrate.

WLI and DIC images for the sol-gel based matrix are shown in Figure 2. Wrinkling of the coating can be observed with the metal substrate apparent beneath in both WLI and DIC images. Cracks and areas of apparent disbondment appear in DIC images, suggesting that the coating matrix is brittle. There are also some bubbles or small droplets present throughout the panel likely due to solvent evaporation during the curing process.

Figure 3 shows that the coating with non-functionalised silica nanoparticles is less brittle than the matrix itself, but nanoparticles are not homogeneously distributed and some porosity is evident. DIC images still show cracks and discontinuity of the coating with non-functionalised silica nanoparticles, even though there has been an increase in homogeneity of the coating with the addition of silica nanoparticles to the matrix formulation.

For the coating with functionalised silica nanoparticles an increase in homogeneity and a decrease in porosity is achieved, which is shown in both WLI and DIC images in Figure 4. This is probably due to the influence of functionalised silica nanoparticles which possibly helps to increase the flexibility of the coatings and also to reduce the internal stress, leading to a more homogeneous coating.

Figure 5 shows the AFM images of the coatings with non-functionalised and functionalised silica. The dark domains are attributed to the silica nanoparticles, which are distributed within the matrix network. Functionalised-silica nanoparticles are better distributed throughout the coating showing an increase in homogeneity, while the coating with non-functionalised silica nanoparticles (Figure 5a) showed some agglomeration and inhomogeneous distribution of nanoparticles in the coating. The improvement in dispersion can be explained by the

functionalisation, which causes steric hindrance avoiding agglomeration of nanoparticles during the incorporation process, and the increased compatibility between the GPTMS grafted on the silica surface and the GPTMS in the matrix network. This can lead to a stronger interface between the matrix and the nanoparticles [18]. The surface treatment also helps to supress agglomeration of the silica nanoparticles due to their enhanced resin-wettability, which is in line with other investigations [34, 35].

3.2 Corrosion performance

Photographs of samples exposed to neutral salt spray are shown in Figure 6. The addition of non-functionalised silica nanoparticles (Fig. 6b, e) improved coating performance compared to the sol-gel based coating matrix itself (Fig. 6a, d), but corrosion is evident after 72 h for these coatings. However, with the incorporation of GPTMS-functionalised silica nanoparticles an improvement of the corrosion resistance can be observed, with very little corrosion even up to 72 h (Fig. 6c, f).

Corrosion potential, E_{corr}, as a function of time is represented in Figure 7. Data was collected (for a duration of 1 h) at times of 1 h, 24 h and 48 h of exposure. All coated samples show a corrosion potential substantially higher than the bare steel (Q-panel), suggesting that these coatings have a barrier effect, in agreement with trends observed by other researchers [36, 37]. At the beginning of the experiment, the coating with non-functionalised silica nanoparticles had a slightly higher potential than the matrix and the coating with functionalised silica. There is a clear drop in all potential values for coated samples up to 24 h. After 24 h, the potential for both the matrix and the coating with non-functionalised silica continues to drop suggesting that corrosion on the sample increases possibly due to water uptake in the coating. An increased anodic activity would shift the corrosion potential in the negative potential direction. Other authors looking at coating resistance have observed such changes in OCP as corrosion occurs through the coating. In contrast, the coating with functionalised silica tends to stabilise after the

24 h, possibly suggesting higher corrosion resistance over all the samples although this needs to be confirmed from EIS measurements.

Immersion tests were performed in 3.5 wt.% NaCl solution for 48 h. Figure 8 shows the impedance spectra for all coating formulations obtained at 48 h. The higher values of impedance for the coating with functionalised silica over the other formulations indicate a clear barrier protection provided with this coating over all. Two time constants can be observed: the high frequency time constant which is associated with capacitance and resistance of the sol-gel coating and the low frequency constant which can be associated to capacitance of the electrochemical double layer on the substrate/electrolyte interface.

Equivalent circuit models were used to fit EIS data allowing for a detailed analysis of physicochemical and electrochemical processes associated with the nature of the corrosion protection offered by the coatings. Figure 9 displays the equivalent circuit used for the fitting of the sol-gel based coatings with and without silica nanoparticles. This circuit is a modified Randles cell where R_s represents the solution resistance, R_{corr} and Q_{dl} are the resistance of the charge transfer and the capacitance of the double layer in the electrolyte solution interface respectively, R_{pore} is the resistance of ion-conducting paths/pores in the coating, and Q_{coat} is related to the intact part of the coatings. Constant phase elements (Q) were used in all fittings instead of ideal capacitors to take into account the fact that the coating is an imperfect dielectric. This is mandatory when the phase angle of capacitor is different from -90° [38].

Impedance values obtained as a function of frequency and equivalent circuit given in Figure 9 were used to find the values of the circuit elements over the duration of the test. Evolution of the calculated parameters like Q_{coat}, R_{corr} and R_{pore} is represented as a function of time to monitor the coating degradation, as shown in the plots in Figure 10, 11, and 12. These values have been normalised to cell exposure area and thickness of the films.

According to some authors, the coating capacitance can be associated with water uptake or entry of the electrolyte into the coating [39, 40]. Figure 10 shows that Q_{coat} values for the samples with silica nanoparticles are lower than the values calculated for the resin itself. For each coating, the increase of the immersion time leads to some coating degradation, reflected in the plot by an increase in Q_{coat}. Nevertheless, Q_{coat} values for the coatings with functionalised silica are about one order of magnitude lower than the coatings with non-functionalised silica and the sol-gel based matrix itself, indicating a significant improvement in the protective behaviour of these coatings over the other formulations.

The other parameter that can be evaluated is R_{pore} which is related to the existence or absence of ion-conducting paths/pores in the coating and an indication of the quality of the coating. R_{pore} is a measurement of the porosity of the film, where a high R_{pore} means that the ion-conducting paths is low, corresponding to a good coating. As seen in Figure 11, the coating with functionalised silica nanoparticles has the highest pore resistance. This behaviour indicated the most effective barrier properties provided by the coating with functionalised nanoparticles.

When the electrolyte comes in contact with the steel surface, electrochemical reactions arise potentially resulting in the formation of corrosion products at the interface. The associated processes are represented by the interfacial resistance, R_{corr}, and the double layer capacitance, Q_{dl}. The protective characteristics of the coatings with nanoparticles is confirmed by the higher values of R_{corr} compared with the resin itself (Figure 12). The highest resistance to corrosion was observed for the coating containing functionalised silica nanoparticles. It can be observed that only this coating presented R_{corr} values above 10^7 $\Omega.cm^2$, which is a requirement to provide effective corrosion protection [41]. Another parameter which indicates this behaviour is the conductivity, which was also calculated and normalised. A decrease in conductivity values from the matrix ($1.6.10^{-5}$ S/cm) to the coating with non-functionalised silica ($1.24.10^{-6}$ S/cm) and still more to the coating with functionalised silica ($4.44.10^{-7}$ S/cm) was observed. It can be

concluded that the addition of silica and more explicitly functionalised silica, leads to a decrease in conductivity, and an increase in resistance, which is related to an improvement in barrier properties of the films.

4. CONCLUSIONS

The present work reports the influence of unfunctionalised and functionalised silica nanoparticles into a sol-gel based matrix and on the corrosion resistance. It was found that the increase in organic content, introduced via the glycidyl group of the GPTMS, in the sol-gel based matrix formulation help to increase the density and the adhesion of the coating to the substrate.

The introduction of non-treated silica nanoparticles led to an improvement of barrier properties which may be due to cracking prevention and reduced porosity. AFM, WLI and DIC images confirmed an increase in homogeneity leading to an enhancement in coating homogeneity after the addition of silica nanoparticles. EIS results are also in agreement with this, showing an increase in R_{pore}, which means that the ion-conducting paths/pores in the coatings is lower, corresponding to a good coating.

When the matrix formulation incorporates silica nanoparticles treated with GPTMS, an improvement is observed in the corrosion protection in the neutral salt spray test in comparison to coatings that use the same silica nanoparticles without functionalisation. This is possibly due to a dispersion improvement and a stronger interface between the matrix and nanoparticles. These results are in line with EIS data, confirming that the addition of the functionalised nanoparticles led to an improvement of the corrosion ability of the sol-gel based coating. These specimens show a smaller number of pits and attacked areas as well as a decrease in porosity when compared with the other formulations.

It can be concluded that the addition of silica nanoparticles helps to increase coating homogeneity and decrease cracking propagation, this leading to an improvement in corrosion

resistance. However when these nanoparticles are surface treated with GPTMS, it is possible that the glycidyl group present in this molecule creates a stronger interface nanoparticle-matrix, suppressing agglomeration of nanoparticles and enhancing not just nanoparticle distribution but also corrosion resistance.

Further work on these nano-enabled coatings will focus on improving the understanding of the interactions of the nano-additives with the sol-gel based matrix and could lead in the future to a new generation of products enhanced by nanotechnology.

Acknowledgements

The author would like to thank the Lloyd's Register Foundation for sponsoring this PhD research and the FCR, TCE and MPF Teams at TWI for their support. The author is also grateful to Chun Wang (University of Leeds) for her help with AFM imaging and to J.C.S. Fernandes (Instituto Superior Técnico, Lisboa, Portugal) for his help with the interpreting the electrochemical impedance results.

[Lloyd's Register Foundation] is a charitable foundation, helping to protect life and property by supporting engineering-related education, public engagement and the application of research.

References

[1] W. Stober, A. Fink, E. Bohn, Controlled Growth of Monodisperse Silica Spheres in the Micron Size Range, J. Colloid Interface Sci. 26 (1968) 62–69.

[2] L.L. Hench, J.K. West, The Sol-Gel Process, Chem. Rev. 90 (1990) 33–72.

[3] M.A. Fardad, Catalysts and the structure of SiO_2 sol-gel films, J. Mater. Sci. 35 (2000) 1835–1841.

[4] S. Zheng, J. Li, Inorganic-organic sol gel hybrid coatings for corrosion protection of metals, J. Sol-Gel Sci. Technol. 54 (2010) 174–187.

[5] J. Malzbender, J.M.J. den Toonder, A.R. Balkenende, G. de With, Measuring mechanical properties of coatings: a methodology applied to nano-particle-filled sol-gel coatings on glass, Mater. Sci. Eng. R. 36 (2002) 47–103.

[6] M.L. Zheludkevich, R. Serra, M.F. Montemor, I.M. Miranda Salvado, M.G.S. Ferreira, Corrosion protective properties of nanostructured sol-gel hybrid coatings to AA2024-T3, Surf. Coatings Technol. 200 (2006) 3084–3094.

[7] H. Rahimi, R. Mozaffarinia, A. Hojjati Najafabadi, R. Shoja Razavi, E. Paimozd, Optimization of process factors for the synthesis of advanced chrome-free nanocomposite sol-gel coatings for corrosion protection of marine aluminum alloy AA5083 by design of experiment, Prog. Org. Coatings. 76 (2013) 307–317.

[8] F. Khelifa, M.E. Druart, Y. Habibi, F. Bénard, P. Leclère, M. Olivier, P. Dubois, Sol-gel incorporation of silica nanofillers for tuning the anti-corrosion protection of acrylate-based coatings, Prog. Org. Coatings. 76 (2013) 900–911.

[9] H. Rahimi, R. Mozafarinia, R.S. Razavi, E. Paimozd, A.H. Najafabadi, Processing and properties of GPTMS-TEOS hybrid coatings on 5083 aluminum alloy, Adv. Mater. Res. 239–242 (2011) 736–742.

[10] R.N. Peres, E.S.F. Cardoso, M.F. Montemor, H.G. de Melo, A. V. Benedetti, P.H. Suegama, Influence of the addition of SiO_2 nanoparticles to a hybrid coating applied on an AZ31 alloy for early corrosion protection, Surf. Coatings Technol. 303 (2016) 372–384.

[11] I. Santana, A. Pepe, E. Jimenez-Pique, S. Pellice, I. Milosev, S. Ceré, Corrosion protection of carbon steel by silica-based hybrid coatings containing cerium salts: Effect of silica nanoparticle content, Surf. Coatings Technol. 265 (2015) 106–116.

[12] A. Phanasgaonkar, V.S. Raja, Influence of curing temperature, silica nanoparticles- and cerium on surface morphology and corrosion behaviour of hybrid silane coatings on mild steel, Surf. Coatings Technol. 203 (2009) 2260–2271.

[13] N. Valipour Motlagh, F.C. Birjandi, J. Sargolzaei, N. Shahtahmassebi, Durable, superhydrophobic, superoleophobic and corrosion resistant coating on the stainless steel surface using a scalable method, Appl. Surf. Sci. 283 (2013) 636–647.

[14] D. Kumar, X. Wu, Q. Fu, J.W.C. Ho, P.D. Kanhere, L. Li, Z. Chen, Development of durable self-cleaning coatings using organic-inorganic hybrid sol-gel method, Appl. Surf. Sci. 344 (2015) 205–212.

[15] M. Myers, Current and impeding developments in silica nanoparticle use in UV-curable systems. PCI. (2011) 28–31.

[16] A. Kukacková, S. as, Using the Si-O strength, Eur. Coatings J. (2007).

[17] R. Zandi Zand, V. Flexer, M.D. Keersmaecker, K. Verbeken, A. Adriaens, Effects of activated ceria and zirconia nanoparticles on the protective behaviour of silane coatings in chloride solutions, Int. J. Electrochem. Sci. 10 (2015) 997–1014.

[18] I.A. Rahman, V. Padavettan, Synthesis of silica nanoparticles by sol-gel: size-dependent properties, surface modification, and applications in silica-polymer nanocomposites. A review, J. Nanomaterials 2012, Article ID 132424, (2012).

[19] Z.Z. Wang, P. Gu, Z. Zhang, L. Gu, Y.Z. Xu, Mechanical and tribological behavior of epoxy/silica nanocomposites at the micro/nano scale, Tribol. Lett. 42 (2011) 185–191.

[20] J. Wang, G. Wu, J. Shen, T. Yang, Q. Zhang, B. Zhou, Z. Deng, B. Fan, D. Zhou, F. Zhang, Scratch-Resistant Improvement of Sol-Gel Derived Nano-Porous Silica Films, J. Sol-Gel Sci. Technol. 18 (2000) 219–224.

[21] A. Zhu, A. Cai, J. Zhang, H. Jia, J. Wang, PMMA-grafted-silica/PVC nanocomposites: Mechanical performance and barrier properties, J. Appl. Polym. Sci. 108 (2008) 2189–2196.

[22] Y. Zhao, N. Dan, Y. Pan, N. Nitin, R. V. Tikekar, Enhancing the barrier properties of colloidosomes using silica nanoparticle aggregates, J. Food Eng. 118 (2013) 421–425.

[23] M.F. Montemor, M.G.S. Ferreira, Cerium salt activated nanoparticles as fillers for silane films: Evaluation of the corrosion inhibition performance on galvanised steel substrates, Electrochim. Acta. 52 (2007) 6976–6987.

[24] M.F. Montemor, R. Pinto, M.G.S. Ferreira, Chemical composition and corrosion protection of silane films modified with CeO_2 nanoparticles, Electrochim. Acta. 54 (2009) 5179–5189.

[25] S. Chen, B. You, S. Zhou, L. Wu, Preparation and characterization of scratch and mar resistant waterborne epoxy/silica nanocomposite clearcoat, J. Appl. Polym. Sci. 112 (2009) 3634–3639.

[26] Y. Bautista, J. Gonzalez, J. Gilabert, M.J. Ibañez, V. Sanz, Correlation between the wear resistance, and the scratch resistance, for nanocomposite coatings, Prog. Org. Coatings. 70 (2011) 178–185.

[27] M.L. Zheludkevich, I.M. Salvado, M.G.S. Ferreira, Sol–gel coatings for corrosion protection of metals, J. Mater. Chem. 15 (2005) 5099–5111.

[28] N.C. Rosero-Navarro, S.A. Pellice, A. Durán, M. Aparicio, Effects of Ce-containing sol-gel coatings reinforced with SiO_2 nanoparticles on the protection of AA2024, Corros. Sci. 50 (2008) 1283–1291.

[29] M. Zaharescu, L. Predoana, A. Barau, D. Raps, F. Gammel, N.C. Rosero-Navarro, Y. Castro, A. Durán, M. Aparicio, SiO_2 based hybrid inorganic–organic films doped with TiO2–CeO2 nanoparticles for corrosion protection of AA2024 and Mg-AZ31B alloys, Corros Sci. 51 (2009) 1998-2005

[30] W. He, D. Wu, J. Li, K. Zhang, Y. Xiang, L. Long, S. Qin, J. Yu, Q. Zhang, Surface modification of colloidal silica nanoparticles: Controlling the size and grafting process, Bull. Korean Chem. Soc. 34 (2013) 2747–2752.

[31] M.E. Orazem, B. Tribollet, Electrochemical Impedance Spectroscopy, ECS, John Wiley & Sons, New York, 2008

[32] R.B. Figueira, I.R. Fontinha, C.J.R. Silva, E. V Pereira, Hybrid Sol-Gel Coatings: Smart and Green Materials for Corrosion Mitigation, Coatings. 6 (2016) 12.

[33] R. Zandi-Zand, A. Ershad-Langroudi, A. Rahimi, Silica based organic-inorganic hybrid nanocomposite coatings for corrosion protection, Prog. Org. Coatings. 53 (2005) 286–291.

[34] R. Eslami-Farsani, H. Khosravi, S. Fayazzadeh, Using-3-glycidoxypropyltrimethoxysilane functionalized SiO_2 nanoparticles to improve flexural properties of glass fibers/epoxy grid-stiffened composite panels, Int. J. Chem. Mol. Nucl. Mater. Metall. Eng. 9 (2015) 1377–1380.

[35] S. Kang, S. Hong, C.R. Choe, M. Park, S. Rim, J. Kim, Preparation and characterization of epoxy composites filled with functionalized nanosilica particles obtained via sol-gel process, Polymer, 42 (2001) 879–887.

[36] M. Longhi, S.R. Kunst, L.V.R. Beltrami, E.K. Kerstner, C.I.S. Filho, V.H.V. Sarmento, C. Malfatti, Effect of tetraethoxy-silane (TEOS) amounts on the corrosion prevention properties of siloxane-PMMA hybrid coatings on galvanized steel substrates, Mater. Res. 18 (2015) 1140-1155.

[37] S.R. Kunst, H.R.P. Cardoso, L.V.R. Beltrani, C.T. Oliveira, T.L. Menezes, J.Z. Ferreira, C.F. Malfatti, New sol-gel formulations to increase the barrier effect of a protective coating against the corrosion and wear of galvanized steel, Mat. Res. 18 (2015) 138-150.

[38] E. Barsoukov, J.R. Macdonald, Impedance Spectroscopy: Theory, experimental and applications, 2nd ed., John Wiley & Sons, 2005

[39] M.G. Olivier, M. Poelman, Use of Electrochemical Impedance Spectroscopy (EIS) for the Evaluation of Electrocoatings Performances, in: Reza Shoja Razavi (Ed.), Recent Res. Corros. Eval. Prot., Intechopen, 2012.

[40] M.L. Zheludkevich, R. Serra, M.F. Montemor, K.A. Yasakau, I.M.M. Salvado, M.G.S. Ferreira, Nanostructured sol-gel coatings doped with cerium nitrate as pre-treatments for AA2024-T3 Corrosion protection performance, Electrochim. Acta. 51 (2005) 208–217.

[41] H. Leidheiser, Electrical and electrochemical measurements as predictors of corrosion at the metal—organic coating interface, Prog. Org. Coatings. 7 (1979) 79–104.

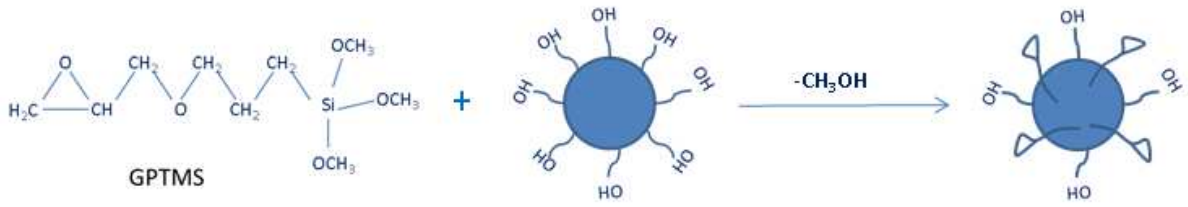

Figure 1. Surface functionalisation of silica nanoparticle with GPTMS 'Courtesy of TWI Ltd.'

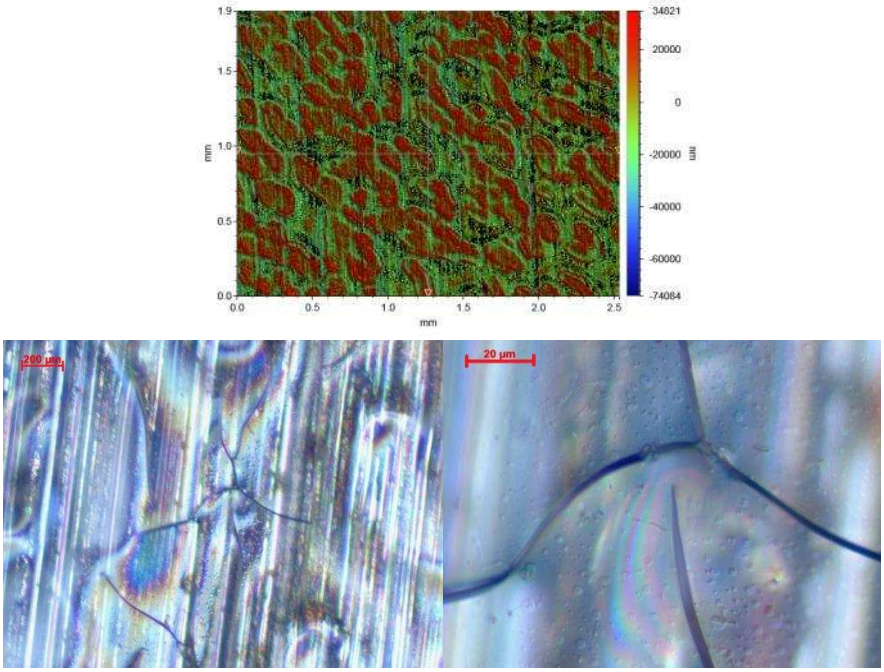

Figure 2. WLI and DIC images for the sol-gel based matrix 'Courtesy of TWI Ltd.'

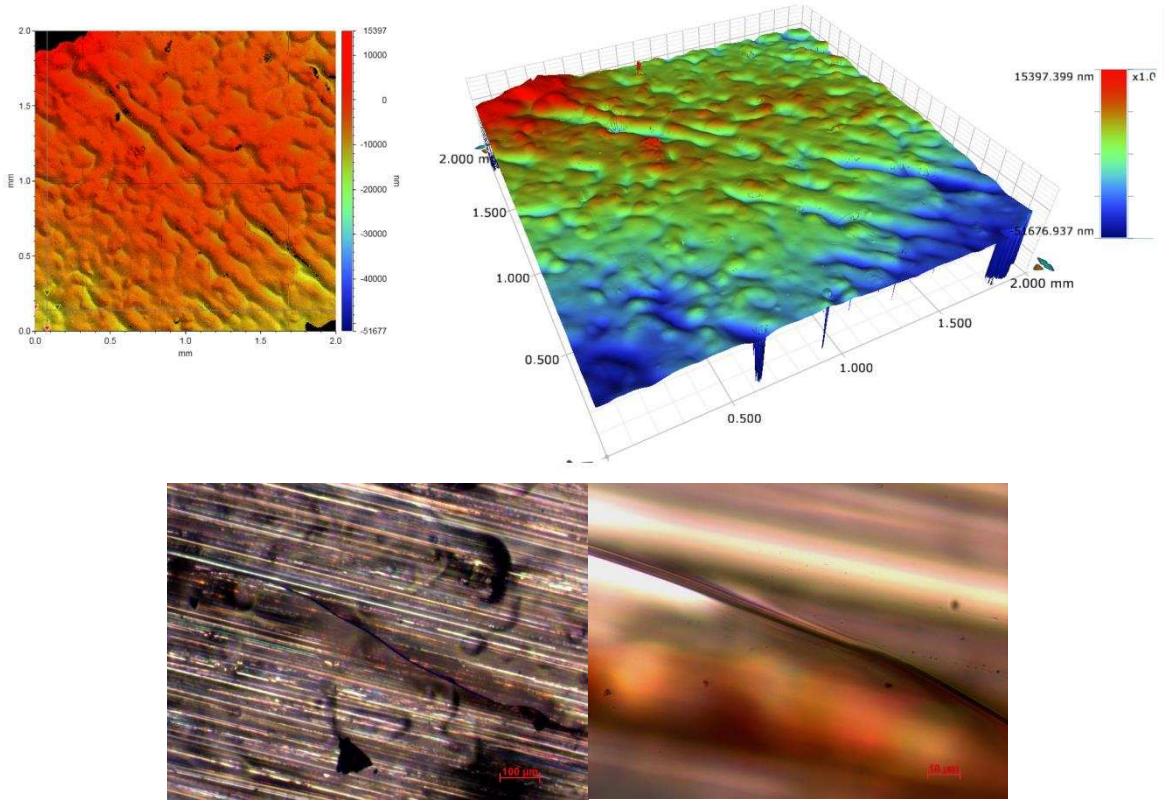

Figure 3. WLI and DIC images for the coating with non-functionalised silica 'Courtesy of TWI Ltd.'

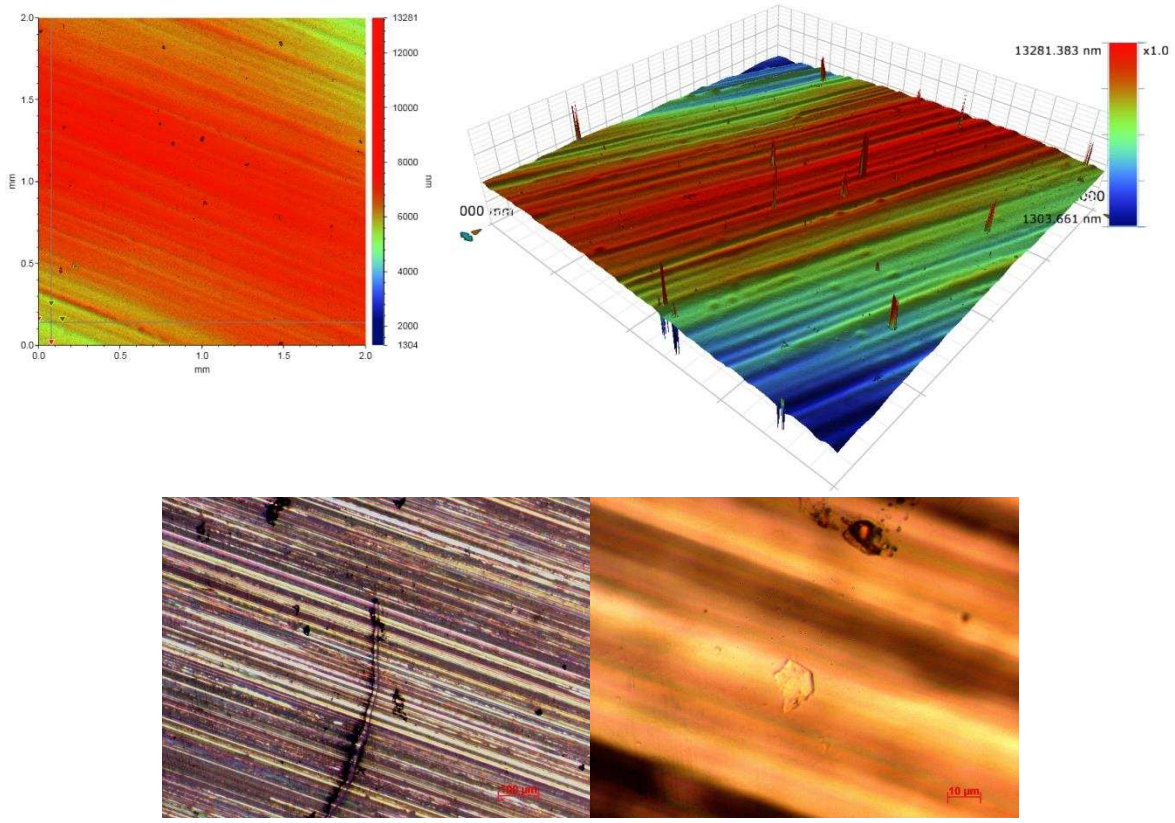

Figure 4. WLI and DIC images for the coating with functionalised silica 'Courtesy of TWI Ltd.'

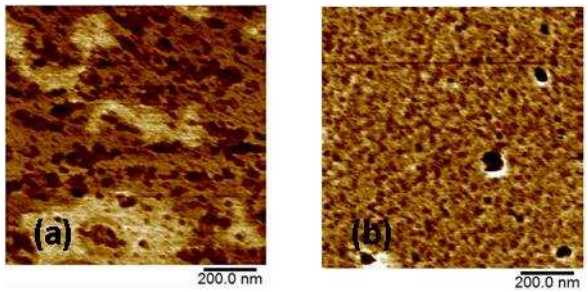

Figure 5. AFM images of nanocoatings: (a) matrix with 10 wt.% non-functionalised silica, and (b) matrix with 10 wt.% functionalised-silica 'Courtesy of TWI Ltd.'

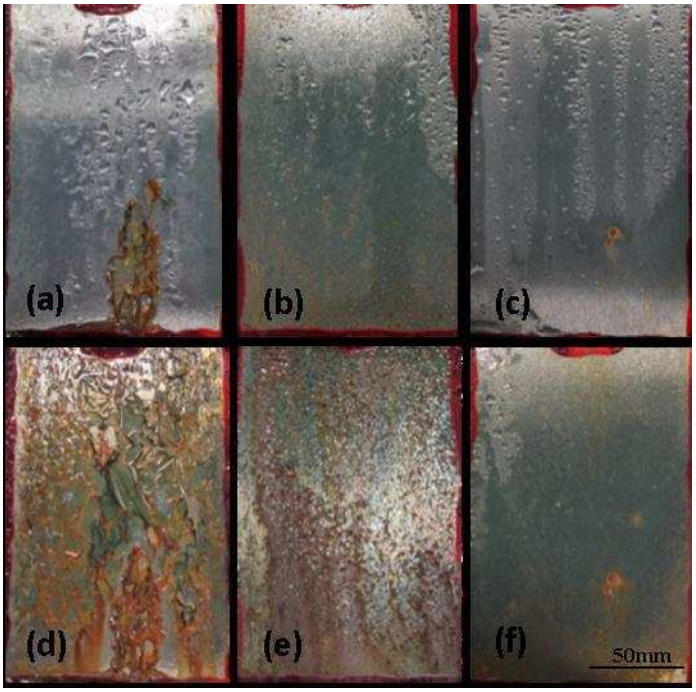

Figure 6. Salt spray results after 24 h (above; a, b, and c) and 72 h (below; d, e, and f). From left to right: sol-gel based matrix (a, d), matrix with 10% non-functionalised silica (b, e), matrix with 10% functionalised-silica (c, f).'Courtesy of TWI Ltd.'

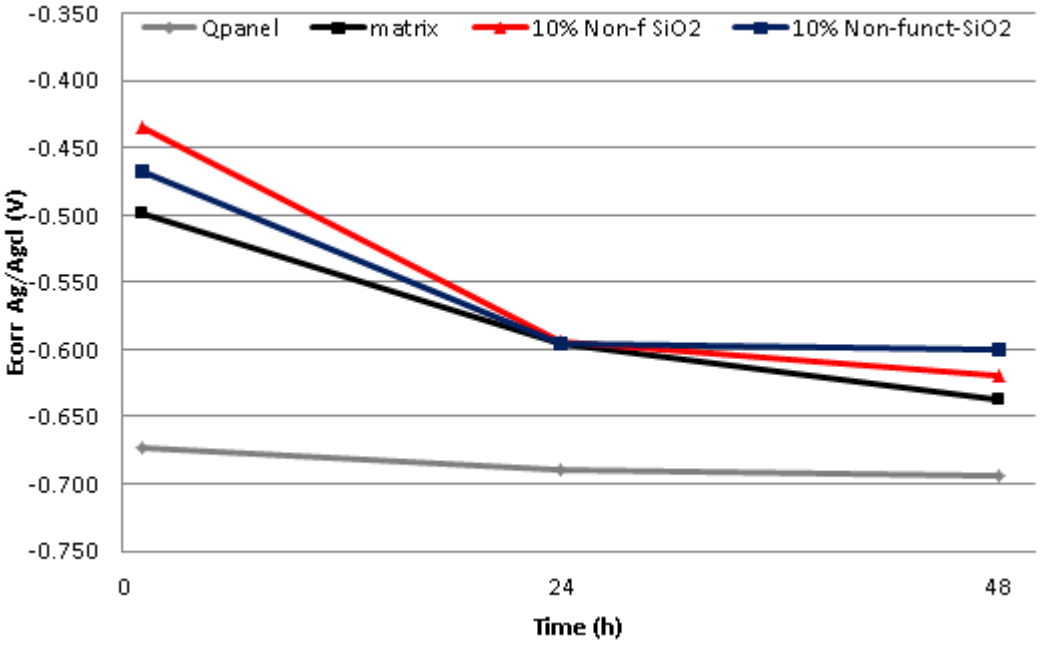

Figure 7. Corrosion potential as a function of time 'Courtesy of TWI Ltd.'

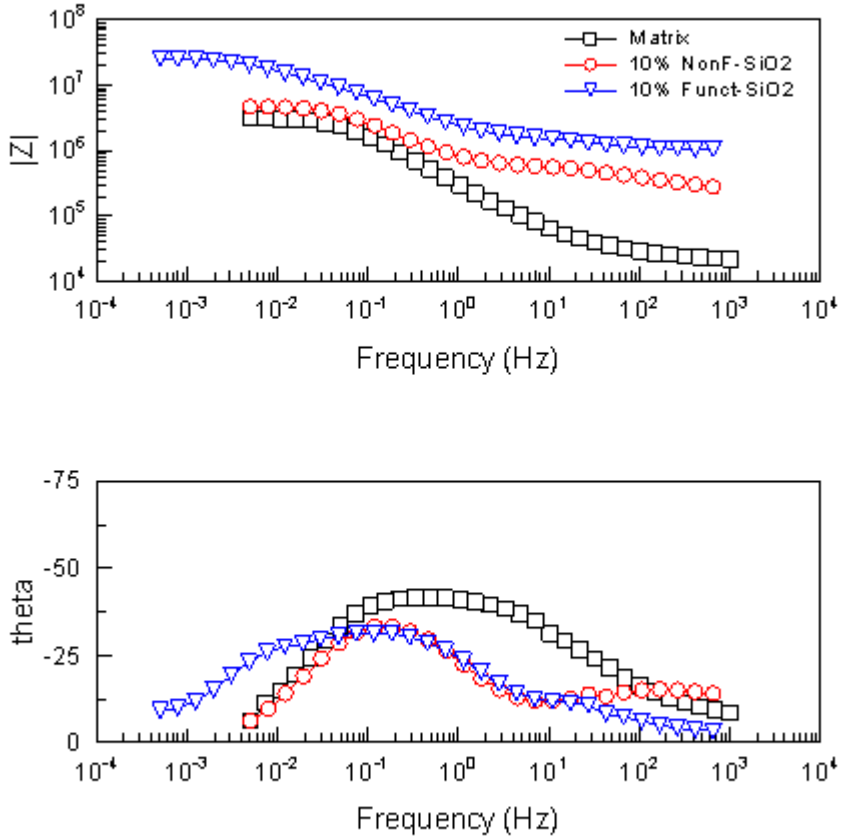

Figure 8. EIS Bode plots obtained for the sol-gel coatings at 48 h 'Courtesy of TWI Ltd.'

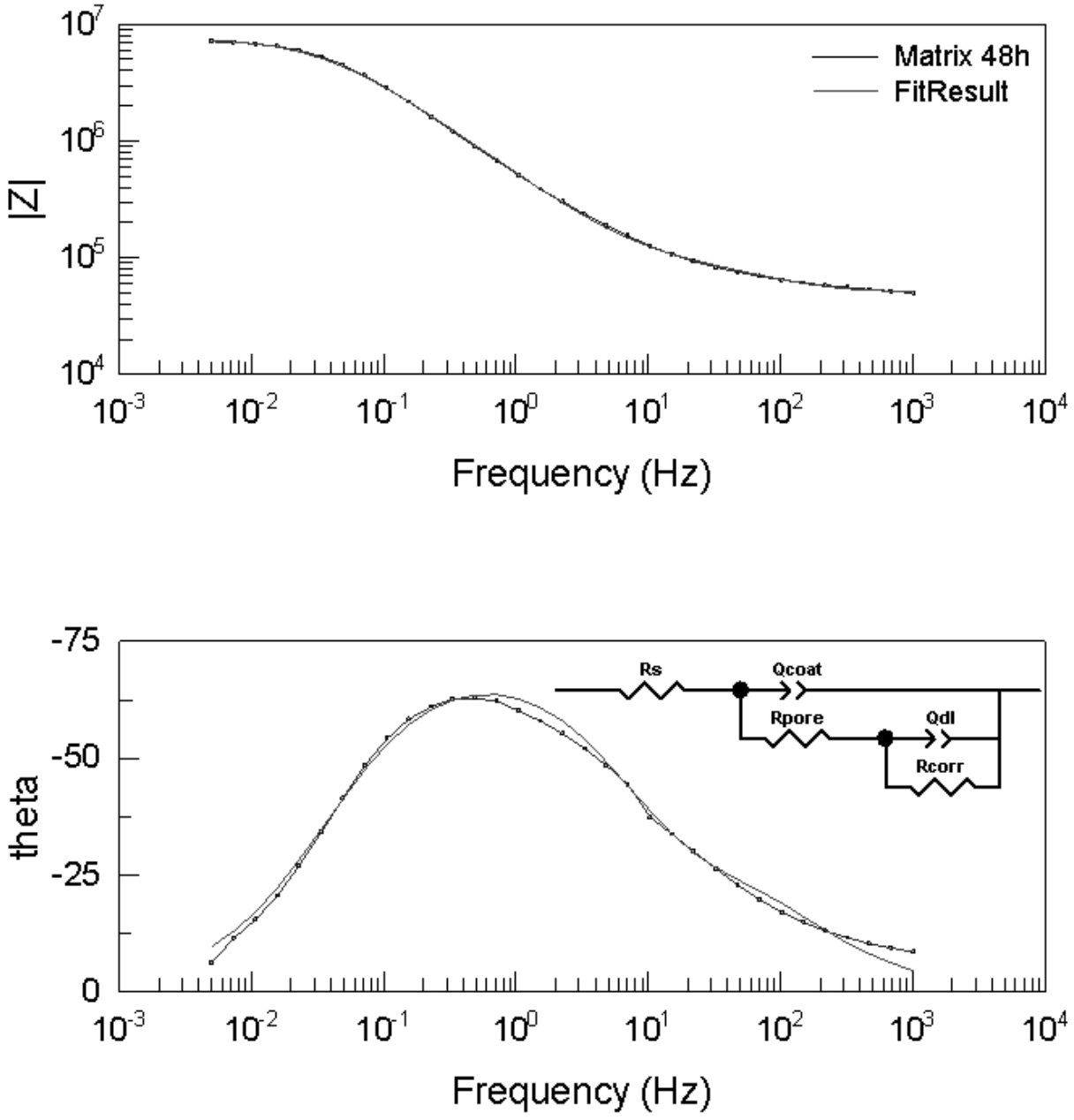

Figure 9. Fitting of the EIS Bode plots for the matrix without nanoparticles. Equivalent circuit used for the fitting is attached. R_s= 2.16E^{+4} Ω.cm; R_{pore}= 3.02E^{+4} Ω.cm; Q_{coat}= 2.97E^{-7} F/cm; n_{coat}= 0.86 ; R_{corr}= 3.35E^{+6} Ω.cm; Q_{dl}= 6.85E^{-7} F/cm ; n_{dl}= 0.81; χ^2= 2.64E^{-3}.

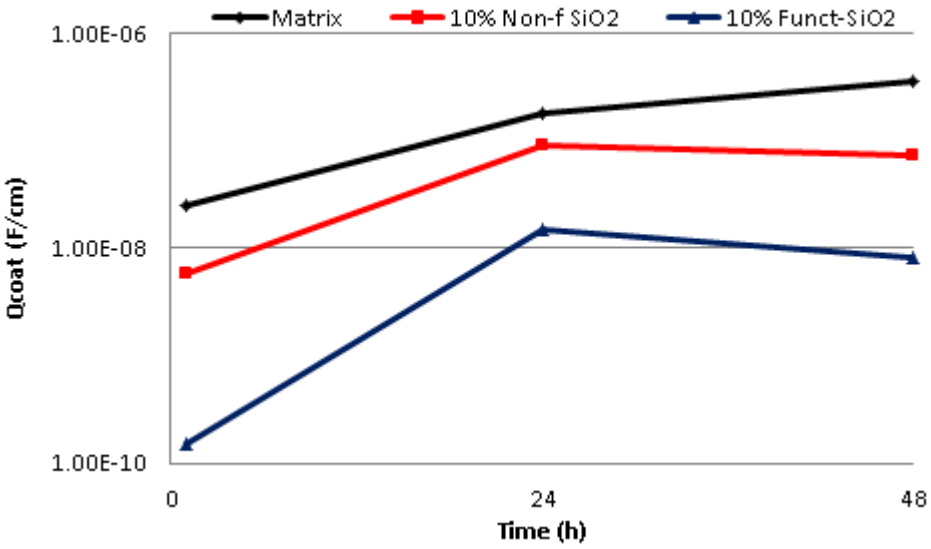

Figure 10. Time dependence of coating capacitance (Q_{coat}) up to 48 h 'Courtesy of TWI Ltd.'

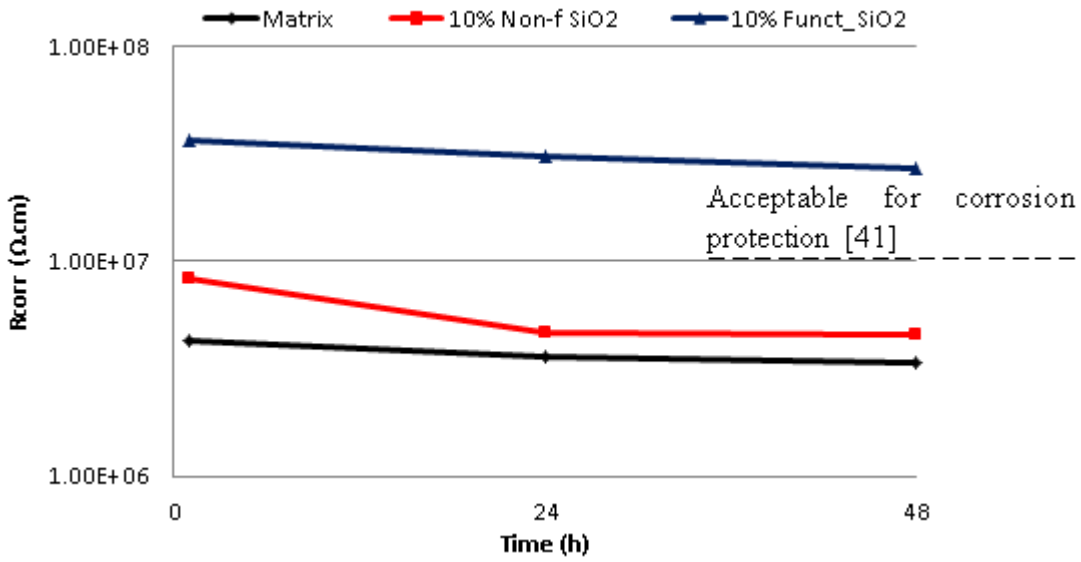

Figure 11. Time dependence of pore resistance (R_{pore}) up to 48 h 'Courtesy of TWI Ltd.'

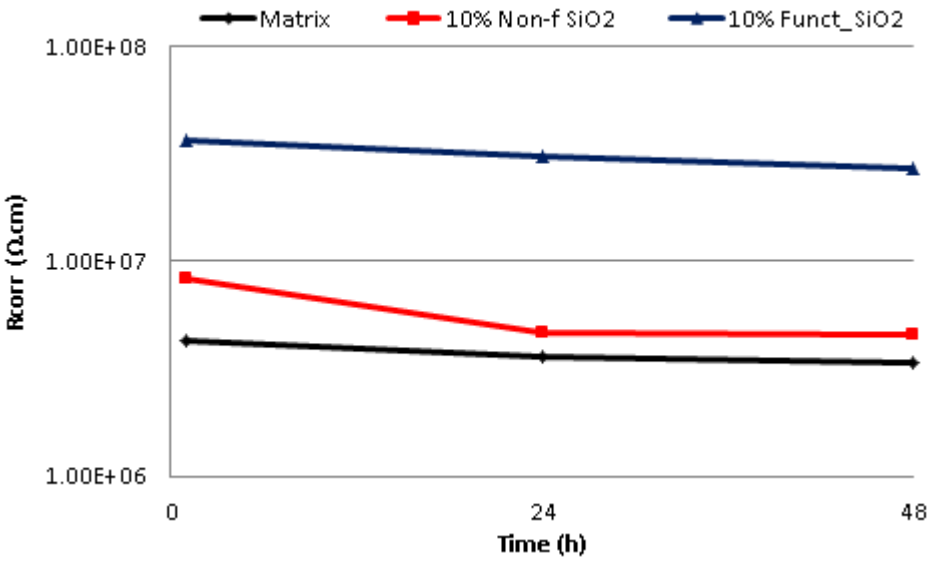

Figure 12. Time dependence of corrosion resistance (R_{corr}) up to 48 h 'Courtesy of TWI Ltd.'

Figure 1. Surface functionalisation of silica nanoparticle with GPTMS 'Courtesy of TWI Ltd.'
Figure 2. WLI and DIC images for the sol-gel based matrix 'Courtesy of TWI Ltd.'
Figure 3. WLI and DIC images for the coating with non-functionalised silica 'Courtesy of TWI Ltd.'
Figure 4. WLI and DIC images for the coating with functionalised silica 'Courtesy of TWI Ltd.'
Figure 5. AFM images of nanocoatings: (a) matrix with 10 wt.% non-functionalised silica, and (b) matrix with 10 wt.% functionalised-silica 'Courtesy of TWI Ltd.'
Figure 6. Salt spray results after 24 h (above; a, b, and c) and 72 h (below; d, e, and f).
From left to right: sol-gel based matrix (a, d), matrix with 10% non-functionalised silica (b, e), matrix with 10% functionalised-silica (c, f) 'Courtesy of TWI Ltd.'
Figure 7. Corrosion potential as a function of time 'Courtesy of TWI Ltd.'
Figure 8. EIS Bode plots obtained for the sol-gel coatings at 48 h 'Courtesy of TWI Ltd.'
Figure 9. Fitting of the EIS Bode plots for the matrix without nanoparticles. Equivalent circuit used for the fitting is attached. R_s= 2.16E^{+4} Ω.cm; R_{pore}= 3.02E^{+4} Ω.cm; Q_{coat}= 2.97^{E-7} F/cm; n_{coat}= 0.86 ; R_{corr}= 3.35E^{+6} Ω.cm; Q_{dl}= 6.85^{E-7} F/cm ; n_{dl}= 0.81; χ^2= 2.64^{E-3} 'Courtesy of TWI Ltd.'
Figure 10. Time dependence of coating capacitance (Q_{coat}) up to 48 h 'Courtesy of TWI Ltd.'
Figure 11. Time dependence of pore resistance (R_{pore}) up to 48 h 'Courtesy of TWI Ltd.'
Figure 12. Time dependence of corrosion resistance (R_{corr}) up to 48 h 'Courtesy of TWI Ltd.'

Table 1. TES40/GPTMS molar ratios combination.

TES40	GPTMS	IMS	HCl	H_2O
1	0.6	1.35	0.18	3.07
1	0.9	1.35	0.08	3.07
1	0.9	2.67	0.75	6.15
1	1.8	2.67	0.75	8.33